

2.18 μm Mid IR emission from highly transparent Er^{3+} doped tellurite glass ceramic for bio applications

R Morea¹, T T Fernandez¹, A Miguel², M Hernandez³, J M Ulloa⁴, J Fernandez^{2,5},
R Balda^{2,5}, J Solís¹, J Gonzalo¹

1. Laser Processing Group, Instituto de Optica, CSIC, Serrano 121, E- 28006 Madrid, Spain

2. Dept. of Applied Physics I, Universidad del Pais Vasco UPV/EHU, Alameda Urquijo s/n, E-48013 Bilbao, Spain

3. Instituto de Estructura de la Materia, CSIC, Serrano 121, E- 28006 Madrid, Spain

4. Institute for Systems Based on Optoelectronics and Microtechnology, Universidad Politécnica de Madrid, E-28040 Madrid, Spain

5. Materials Physics Center CSIC-UPV/EHU and Donostia International Physics Center, E-20080 San Sebastian, Spain

e-mail address: j.gonzalo@csic.es

Abstract: Intense emission peaking at 2.18 μm was successfully obtained from erbium upon rigorous engineering of its glass host. Highly localized crystallization of erbium sites is substantiated by micro Raman and micro-PL along with TEM.

OCIS codes: 250.5230 Photoluminescence; (160.5690) Rare-earth-doped materials; 160.2750 amorphous materials

The 2.0-2.3 μm wavelength window opens a large opportunity for ground breaking biological applications such as bloodless surgery, non-invasive blood constituents monitoring, high sensitivity tracing of green house gases [1]. For this purpose, room temperature operated high power devices are entering the market of which rare-earth (RE) doped devices hold a prominent place. But such devices are majored by thulium and holmium doping, sidelining erbium. Though Er^{3+} has an active transition to achieve broad 2.0 μm emission, it is usually quenched in an amorphous matrix and hence rarely reported in glasses [2]. However, the use of Er^{3+} as the active ion backbone would leverage efforts and investments done in the telecom industry to non-telecom applications for quick progression. In this work we have successfully engineered a way through which the key 2.0 μm emission was obtained by a specific selection of precursors and customized heat treatment of an Er^{3+} doped tellurite glass. Characterization was carried out using micro-Raman, micro-Photoluminescence and TEM.

Crystallization of an amorphous matrix employing solely thermal treatment cycle sometimes affects the transparency of the glass matrix due to uncontrolled and delocalized crystallization. But if a perfect balance of nucleation rate and growth of nucleus is ensured and maintained, highly localized but well dispersed nanocrystals are formed without degrading the optical transparency. RE fluorides are known to act as nucleation agents in a glassy matrix. The excess addition of erbium fluoride (ErF_3) could even induce a scenario to avoid synthesizing a fully amorphous glass phase [3]. Hence the selection of ErF_3 as a precursor was one of the key element for the administered crystallization of the amorphous matrix that was chosen to be a fluorotellurite glass with a maximum phonon energy of $\sim 850 \text{ cm}^{-1}$ and a optical transparency up to $\sim 6 \mu\text{m}$ [4]. The precursor fluorotellurite glass ($74.6\text{TeO}_2-8.8\text{ZnO}-16.6\text{ZnF}_2$ mol% doped with 1 wt% ErF_3) was prepared by conventional melt quenching. After quenching, a two step heat treatment was carried out to nucleate a glass-ceramic (GC) phase. The first treatment was done at a temperature close to the glass transition temperature ($T_g \approx 293 \text{ }^\circ\text{C}$) for 10 hours, followed by a 3 hours treatment at a temperature slightly below that of the onset of crystallization. After the treatment the GC remained highly transparent.

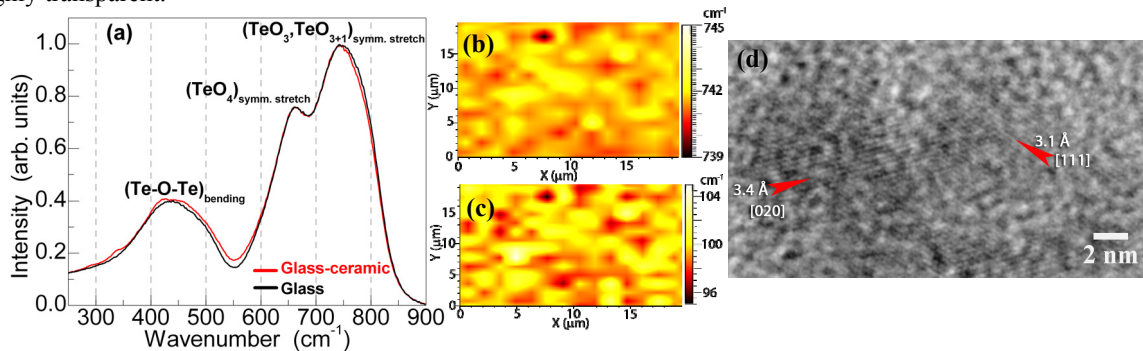


Figure 1 (a) Raman spectra of Glass and Glass ceramic bulk (b) 20 μm x 20 μm mapping of 742 cm^{-1} peak shift (c) 20 μm x 20 μm mapping of variation in FWHM of 742 cm^{-1} peak (d) Lattice planes of ErF_3 crystals in TEM marked with their respective orientations and planes.

Micro-Raman analysis was carried out to find microcrystallization due to heterogeneous nucleation that could affect the transparency or induce color-centers which are undesirable for stable photonic devices. Raman spectra were collected in the 250-900 cm^{-1} spectral region using a confocal Raman microscope (Renishaw inVia) equipped with a He-Cd laser emitting at $\lambda_{\text{exc}} = 442 \text{ nm}$ that was focused on the samples using a 50x magnification objective (spectral resolution: 2 cm^{-1}). Figure 1 compares the Raman spectra for glass and GC samples indicating almost

similar glass network for both except for the subtle shoulders peaking at ~ 290 , ~ 340 and $\sim 420 \text{ cm}^{-1}$ which can be attributed to the ErF_3 nanocrystals present in the GC. Rest all the main band peaks remain unaffected upon crystallization. A 2D mapping of the whole spectra was done over a $20 \times 20 \mu\text{m}^2$ area and the main peak shift and FWHM were plotted in Fig. 1 b&c. Results suggest a homogenous crystallization with almost no discontinuities in the glass matrix. The maximum variation obtained was for the symmetric stretch of Te-O bonds in TeO_{3+1} and TeO_3 units (742 cm^{-1}) which was $\pm 3 \text{ cm}^{-1}$ for peak wavenumber (Fig.1 b) and $\pm 5 \text{ cm}^{-1}$ for the FWHM (Fig.1c).

Micro PL probed the active rare-earth sites of the glass matrix. Strong evidence of site-specific crystallization was obtained. $^2\text{H}_{11/2}$ (522 nm) and $^4\text{S}_{3/2}$ (544 nm) Er^{3+} transitions to its ground state ($^4\text{I}_{15/2}$) [5] were analysed after 980 nm laser excitation. These hypersensitive transitions are ideal for probing RE environment. $^2\text{H}_{11/2}$ transition is sensitive to local site symmetry whereas the $^4\text{S}_{3/2}$ provides indication about changes in the coordination environment [6]. $^2\text{H}_{11/2}$ band remained almost unchanged, whereas major changes were observed for the $^4\text{S}_{3/2}$ band emission indicating that the local site symmetry is least affected compared to the coordination environment. In the GC spectrum (Fig. 2b) the high energy sub-band splitting of $^4\text{S}_{3/2}$ is quenched and shows more Stark splitting compared to its low energy counterpart. The additional Stark splitting of this level indicates the presence of Er^{3+} in sites with lower phonon energy. The formation of ErF_3 nanocrystals was finally confirmed by TEM (Fig 1d).

The presence of ErF_3 nanocrystals has a strong effect in the visible emission of the Er^{3+} ions. From comparing figure 2 a&b it is evident that red emission in the GC ($^4\text{F}_{9/2}$) is dramatically enhanced. We believe this is due to the co-operative energy transfer between Er^{3+} ions because of shorter inter-ionic distances in the crystalline environment. The population of $^4\text{F}_{9/2}$ level by energy transfer in the GC is in fact the basis of the generation of the $2.0 \mu\text{m}$ emission from the amorphous matrix without leading to fluorescence quenching. $^4\text{F}_{9/2} \rightarrow ^4\text{I}_{11/2}$ emission from the GC is shown in figure 2d whereas figure 2c shows the quenching of the same emission in the glass matrix.

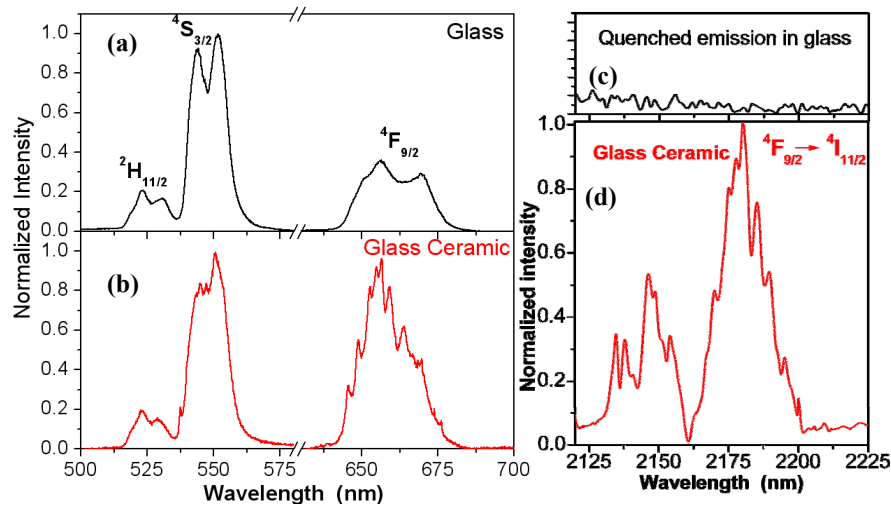


Figure 2. Green and red emissions from (a) Glass (b) Glass ceramic. The Mid-IR emission (c) quenching in glass (d) in Glass ceramic.

The $2.18 \mu\text{m}$ emission from the GC having exactly the same the phonon energy as the glass (850 cm^{-1}) is a potential candidate for high power laser applications and owing to the importance of the wavelength, it could be used to develop photonic devices that works in the $2.0\text{-}2.3 \mu\text{m}$ wavelength window which has high applicability for biomedical, biochemical, biotechnological applications. In conclusion, we have successfully engineered a $2.18 \mu\text{m}$ emission from an amorphous matrix by site-specific nucleation technique. Er^{3+} sites were crystallized to form ErF_3 nanocrystals, this triggered the population of $^4\text{F}_{9/2}$ level leading to intense $^4\text{F}_{9/2} \rightarrow ^4\text{I}_{11/2}$ emission peaking at $2.18 \mu\text{m}$.

References

- [1] Editorial, "Extending opportunities," *Nat Photon*, **6**, 407-407 (2012).
- [2] T. Schweizer, D. Brady, and D. W. Hewak, "Fabrication and spectroscopy of erbium doped gallium lanthanum sulphide glass fibres for mid-infrared laser applications," *Optics Express*, **1**, 102-107 (1997).
- [3] M. Mortier and G. Dantelle, "Oxyfluoride Transparent Glass Ceramics," in *Functionalized Inorganic Fluorides*: John Wiley & Sons, Ltd, pp. 273-305.
- [4] T. T. Fernandez, S. M. Eaton, G. Della Valle, R. M. Vazquez, M. Irannejad, G. Jose, A. Jha, G. Cerullo, R. Osellame, and P. Laporta, "Femtosecond laser written optical waveguide amplifier in phospho-tellurite glass," *Optics Express*, **18**, 20289-20297 (2010).
- [5] A. Miguel, R. Morea, J. Gonzalo, M. A. Arriandaga, J. Fernandez, and R. Balda, "Near-infrared emission and upconversion in Er^{3+} -doped $\text{TeO}_2\text{-ZnO-ZnF}_2$ glasses," *Journal of Luminescence*, **140**, 38-44.
- [6] T. Toney Fernandez, P. Haro-González, B. Sotillo, M. Hernandez, D. Jaque, P. Fernandez, C. Domingo, J. Siegel, and J. Solis, "Ion migration assisted inscription of high refractive index contrast waveguides by femtosecond laser pulses in phosphate glass," *Optics Letters*, **38**, 5248-5251 (2013).